



Effect of nanoparticles on the nucleation and agglomeration rates of hydrate growth using THF–water clathrates

Syed Y. Nahri¹ · James L. Nielsen¹ · Yuanhang Chen¹

Received: 5 February 2019 / Published online: 8 November 2019
© The Author(s) 2019

Abstract

Four types of nanoparticles, amorphous carbon, iron III oxide, SiO₂, and amino-coated SiO₂, were tested to determine changes in tetrahydrofuran–water (THF–water) clathrate hydrate nucleation and agglomeration. Rates were experimentally found to determine their viability for preventing natural gas hydrates from developing during offshore drilling operations. THF–water clathrates were chosen as a model to represent gas hydrate growth at atmospheric pressure. Concentrations of each nanoparticle between 0.15% and 1.0% by weight were tested as a kinetic inhibitor to hydrate formation. Tests were repeated at various temperatures below the formation temperature of 4.4 °C for THF–water clathrate hydrates. Measurements were made to identify how the concentration of THF affects the clathrate hydrates forming under static conditions between 20% and 30% by mole of THF. The primary tests in this study were performed using a 20:80 THF/water ratio. Temperature increases during hydrate nucleation for THF–water were measured between –5 and 3 °C. The range of ideal nanoparticle concentrations was found to be between 0.15% and 0.45% by weight for optimal static, kinetic inhibition of hydrate nucleation. At approximately 0.3% by weight, the most significant inhibition was observed under static conditions for all four types of nanoparticles tested. We found that functionalized amino-coated SiO₂ nanoparticles, across all tests, significantly increased the time required for the formation of THF–water clathrate hydrates compared to the other three non-functionalized nanoparticles. The amorphous carbon and iron III oxide nanoparticles performed similarly across each test and were both the least effective in their inhibition of the clathrate hydrates of the four nanoparticles studied compared to a control.

Keywords Nanoparticles · Gas hydrates · Clathrates · Hydrate inhibition · Functionalized nanoparticles

1 Introduction

The formation of gas hydrates during offshore drilling in deep waters is a well-recognized operational hazard. Drilling through hydrate-bearing sediments (HBS) is frequently encountered to reach deeper hydrocarbon zones or while drilling through HBS to produce natural gas commercially from methane gas hydrates (Grover 2008). The stability of gas hydrates offshore in specific zones has been seen to extend up to 7000 ft below the mud-line and can begin to grow and plug critical well-control equipment such as the blowout preventer (BOP) stack, choke and kill lines which

can lead to severe well-control problems (Kim et al. 2007). Another major issue arises due to the dissociation of HBS during drilling operations when they come in contact or are penetrated by drilling fluids that bring about a change in their temperature and pressure conditions (Kjaer 2014; Zerpa 2013). This leads to severe mud gasification, partial washout and caving, casing running problems and casing subsidence. Models can be used to predict how the drilling fluids will interact with these HBS due to the change in temperature distribution and therefore dissociating more substantial amounts of gas within the wellbore. Wang et al. (2019) proposed an improved thermal model for predicting the temperature distribution in gas-dominated systems by considering the influences of hydrate behavior on the variation in temperature. Once the gas has entered the drilling fluid column, it can then begin to reform into methane hydrates.

There are various ways by which methane hydrates can be prevented. Thermodynamic hydrate inhibitors (THI) can

Edited by Yan-Hua Sun

✉ Yuanhang Chen
ychensu26@gmail.com

¹ Craft and Hawkins Department of Petroleum Engineering, Louisiana State University, Baton Rouge, LA 70803, USA

be used to alter the chemical potential of the aqueous or hydrate phase at high THF concentrations. When THI are present, the hydrate dissociation curve displaces to lower temperatures or higher pressures. One of the most popular methods of shifting the thermodynamic equilibrium of hydrate growth is through the use of pumping large amounts of methanol and propylene and ethylene glycols into the troubled zones known for hydrate development (Ameripour 2005). Bishnoi et al. used clathrate hydrate models to determine how electrolytes would be able to affect the rate of hydrate development (Bishnoi and Dholabhai 1999). They found that large concentrations of salts were required. Weight percentages of salt in the fluids ranging from 5% to 15% were required to significantly inhibit the rate of hydrate growth. Many thermodynamic inhibitors were found to have multiplicative effects on the rate of hydrate growth when they combined together. When testing these different hydrate inhibitors, Sloan (1990) tested how each affected the rate of hydrate growth and also combined the different inhibitors to see whether the effects were the same. Their results showed that when each inhibitor was used, they individually performed well at inhibiting the growth of hydrates; however, when they were combined, the effects were magnified and the performance was significantly increased.

The other method of preventing hydrates is the application of kinetic hydrate inhibitors (KHIs) which are added at low concentrations and do not affect the thermodynamics of hydrate formation (Meindinyo 2017). Instead, KHIs may delay hydrate nucleation and crystal growth. Anti-agglomerates are also used at low concentrations to prevent the agglomeration of hydrates so that the hydrate crystals are transportable through the well before forming a plug. These inhibitors are generally used in conjunction with each other in the right proportions to compose suitable mixtures to form hybrid inhibitors (Pakulski 2011). At extreme water depths or extremely low mud-line temperatures, thermodynamic inhibitors by themselves are not very useful and hence

need to be used in combination with other inhibitors. Such a combination is generally referred to as hybrid inhibitors.

1.1 Hydrate clathrate structure

Hydrates are formed by hydrogen-bonded water molecules interconnecting to form a cage built with pentagonal or hexagonal faces around a cavity which has the capability of encapsulating a central guest molecule (Birkedal 2009; Catak 2006). As shown in Fig. 1, there are two primary types of hydrates, Type 1 and Type 2. A third type, Type H exists but is rarely found in nature. For this study, we will investigate the effects of different nanoparticles which act as kinetic hydrate inhibitors using a close analog to methane hydrates, tetrahydrofuran-water (THF–water) clathrate hydrates. These hydrates are classified as Type 2 hydrates because they are comprised of 136 water molecules, whereas typical methane hydrates are classified as Type 1 hydrates using 46 water molecules to build the crystal structure that can encapsulate a guest molecule (Abay 2011). Hydrate clathrates can form and exist with several different molecules. In this study, we will focus on THF–water and methane–water clathrates, but other combinations exist such as CO_2 –water and H_2 –water clathrates (Xu et al. 2013). Recently, rather than the disruption of hydrates to prevent their formation, the induced development of hydrates has been a means for industries to filter and remove CO_2 and other greenhouse gasses from power plants which rely on coal and natural gas (Li et al. 2011).

The objective of this study is to investigate the effect of nucleation and agglomeration times on clathrate hydrate formation in the presence of nanoparticles (NPs) at varying concentrations. Nanoparticles are particles between 1 and 100 nm in size. NPs have been proven to enhance rheological properties of drilling fluids or enhance rheological properties of drilling fluids under high-pressure/high-temperature conditions, increase wellbore stability

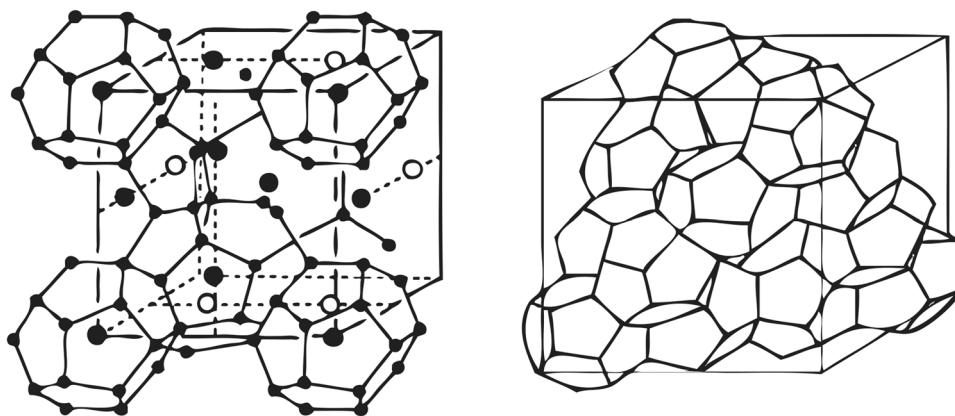


Fig. 1 Crystal structures of Type 1 (left) and Type 2 (right) clathrates (Catak 2006)

and to control or prevent loss circulation (Agarwal et al. 2013). They have been proven to be highly effective while drilling through shale formations because fluid invasion is considerably reduced so there is minimal shale swelling (Amanullah and Al-Tahini 2009).

1.2 Functionalized nanoparticles

Apart from the conventional NPs used, a modified NP coated with amino groups was selected to investigate how functionalized particles can affect the rates of hydrate nucleation and agglomeration. Previous studies have identified how different functional groups on molecular inhibitors can drastically affect the rates of hydrate growth (Anderson et al. 2005). As a comparison in this study, standard SiO₂ nanoparticles will be compared to functionalized SiO₂ nanoparticles that have a double layer of amino groups around the exterior of the particles. Other studies have shown how molecules with organic functional groups have been successfully able to inhibit the formation of hydrates in drilling fluids used for deepwater wells (Halliday 1998).

Tests were conducted using a mixture of tetrahydrofuran (THF) in the presence of deionized water, and the results obtained based on the nucleation time of hydrates will help comprehend the interaction of nanoparticles on the formation of hydrates. This helps develop a guideline on whether currently used nanoparticles lead to inhibition or stability of hydrates over a range of temperatures and concentrations.

1.3 Comparison of methane hydrates to THF hydrates

The primary benefit of using THF–water Type 2 hydrates is that the hydrates are stable at standard pressure and begin growing below 4.4 °C (Lee et al. 2007). It has been reported in previous studies that THF–water hydrates have physical properties very similar to methane hydrates, so they make an excellent analog for testing reagents and materials for inhibiting their formation (Lee et al. 2007). Although each hydrate is of a different structure, Type 1 versus Type 2, their formation and properties are coincidentally similar. This study is to be used as a means of determining possible candidates of hydrate inhibition for methane hydrate experiments. There are so many possible materials that can be used, and therefore, it is important to be able to screen likely candidates to be used as possible additives during drilling operations. Because of the similarity in structure and mechanism of crystal growth, the THF hydrates can help with the screening process for larger-scale studies using methane hydrate flow loops to study natural gas hydrates.

2 Experimental materials

Four different types of nanoparticles were used in this study: iron III oxide (Fe₂O₃), alpha geometrical structured (99% purity, 20–40 nm), amorphous carbon (40 nm), SiO₂ (99.5% purity, 20 nm), and SiO₂ which was coated with two layers of functionalized amino groups, illustrated in Fig. 2 (10–20 nm, surface area of 60–100 m²/g). These amino-coated SiO₂ nanoparticles were referred to as SiO₂+A in this paper. All nanoparticles used in this study were from US-Nano. Deionized (DI) water was used for suspending the nanoparticles and blended with anhydrous THF containing 250 ppm BHT (butylated hydroxytoluene) as an inhibitor, from Sigma-Aldrich. The BHT inhibitor is added by the manufacturer to prevent oxidation of the THF solution. There are no known complications with hydrate development due to the presence of this additive. A Q-Sonica Q500 ultrasonicator was used for the dispersion of all dry solid nanoparticles in this experiment. A 1-L waring commercial blender with mixing speeds of 18,000–22,000 rpm and a magnetic stirrer were both used for additional mixing.

A PolyScience PD15R-40-A11B refrigerated recirculating bath using propylene glycol was used to provide controlled temperatures for the THF and nanoparticle dispersions to produce clathrate hydrates. To record the rate of clathrate hydrate formation, a 1080p webcam was mounted above the recirculating bath to precisely record when the clathrate hydrate begins inducing and agglomeration. SkyStudioPro freeware software was used as a means of taking time-lapse videos with the camera to be used for analysis (Fig. 3).

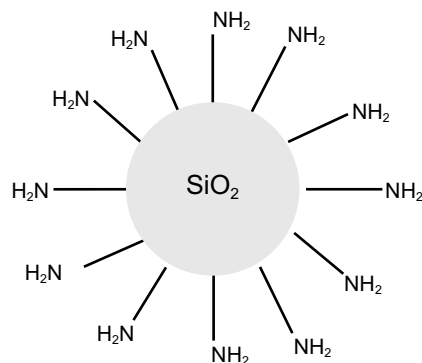


Fig. 2 Representation of a SiO₂ nanoparticle with amino functionalization groups coated around the exterior of the particle



Fig. 3 Q-Sonica Q500 ultrasonicator in a sound enclosure (left) and PolyScience temperature-controlled bath (right)

3 Experimental methods

3.1 Preparation of nanoparticle dispersions

To prepare each nanoparticle dispersion, 200 mL DI water and dry nanoparticles, which were measured using a scale, were added to a flask. The flask was submerged in an ice bath to prevent the solution from heating up while sonicated. During sonication, extreme heating occurs due to localized cavitation bubbles. Prolonged production of these cavitation bubbles results in bulk heating of the solution and lead to excessive evaporation (Taurozzi 2012). The nanoparticle solutions were ultrasonicated using the Q-Sonica Q500 ultrasonicator for 45 min at 50% amplitude pulsing for 1 min on and 15 s off. Once dispersed, the water-nanoparticle solution and THF were both cooled to 5 °C using the recirculating bath before combining each in a 325-mL flask using the magnetic stirrer. Cooling the THF and the water-nanoparticle dispersions before mixing was found to be an essential step in the mixing process

because the addition of concentrated THF to water is very exothermic. When mixing each solution together at 20 °C, we identified, on average, a 5 mL change in total volume. When cooling both the dispersion and the THF prior to mixing, there was no noticeable loss in the total volume. The nanoparticle dispersion and THF were then mixed for 5 min before transferring the solution back to the recirculating bath to begin observations of clathrate hydrate growth at various temperatures.

It is important for this study that the procedure for the nanoparticle dispersions produces a consistent and homogeneous solution that remains stable for long periods of time. To ensure that the dispersions we produced remain fully dispersed, samples were allocated from the 1% (by weight) nanoparticle dispersions and decanted into 8-mL test tubes. The test tubes were placed in a rack with parafilm and tape over the opening to prevent evaporation. Each sample was observed undisturbed for 1 week. As shown in Fig. 4, the nanoparticle dispersions remain homogenous and consistent throughout the full duration of this analysis.

3.2 Distinguishing the phases of hydrate clathrate development

To determine when the THF–water and nanoparticle solutions begin to develop into hydrate clathrates, the developments can be visually determined by the forming clathrate crystals. As the hydrate clathrates begin the nucleation period, the solution undergoes a rapid and sudden conversion from a liquid to a liquid–solid phase. On the time-lapse videos, the nucleation times begin when the solutions reaches 4.4 °C, the temperature at which hydrates begin to develop. Slightly before complete induction occurs, initial crystals can be observed growing out in planar spires on the surface of the solution. As these first nucleated crystals grow across the surface, they will begin to exponentially grow and cause a phase change throughout the beaker. At

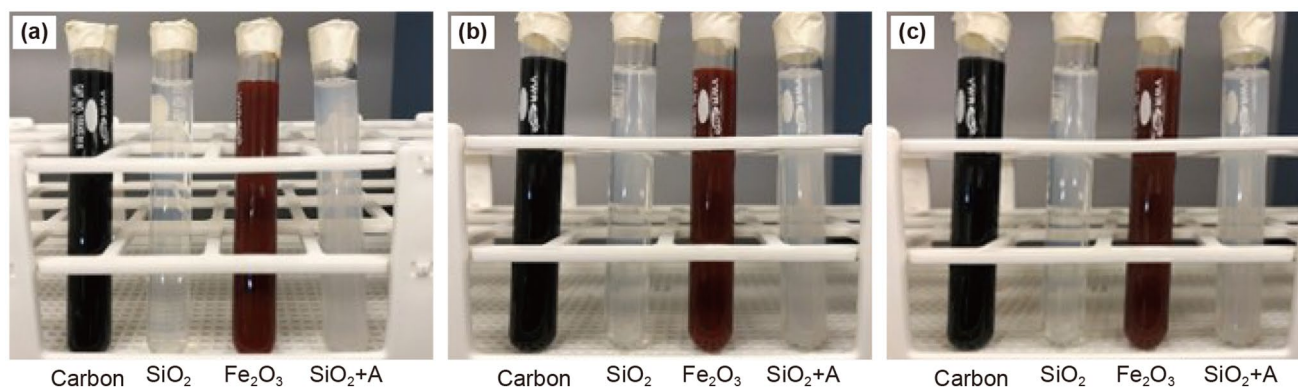


Fig. 4 Nanoparticle dispersions for each of the four nanoparticles in DI water at 1.0 wt% at 0 h (a), 24 h (b), and 168 h (c) from when the solution was initially made

this stage, the solution has both solid and liquid phases that exist together and is visually opaque. The agglomeration stage can be identified when solid hydrate clathrates begin forming around the edge of the beaker and slowly growing inward toward the center. The agglomeration period commences when the entire solution has become solid within the beaker. Each of these stages is displayed in Fig. 5.

The time required for nucleation can be artificially reduced by introducing a seed crystal or promoting their growth by scratching the inside glass of the container the solution is in. Artificially inducing this rapid phase shift can be done within a few seconds using either of these two methods when below 4.4 °C. Previous experiments have shown that the length of the nucleation time is dependent on the apparatus setup, the presence of substrate material, the history of the water, water and gas composition, pressure and temperature, cooling rate, and if it is in a dynamic or static condition (Birkedal 2009). As a result, the nucleation time is sometimes considered a stochastic process. To ensure reproducibility in our study and prevent external influences, each of the tests measuring nucleation times involved allowing the solutions to remain isolated without any external influences once placed in the recirculating bath until they had completely agglomerated. Each test was repeated four times to ensure consistency in results.

3.3 Effect of THF–water molar ratio on nucleation time

For THF–water clathrate hydrates to form, the required minimum molar ratio of THF to water is 1:17 (Lee et al. 2007). The thermodynamics of clathrate hydrate nucleation will become unfavorable at high concentrations of THF relative to water (Nesterov and Reshetnikov 2015). For this study, it was essential to determine whether there was a significant difference between the nucleation times for each nanoparticle solution at different molar ratios of

THF to water. Three molar ratios of THF to water, 20:80, 25:75, and 30:70, were selected, and each was tested using the four types of nanoparticles at 0 °C. Initial tests performed using the required minimum molar ratio of 1:17 was found to require very long periods of time before nucleation occurred. When we increased the THF concentration, we found the nucleation times to be much more reasonable for conducting multiple tests. The 20:80 molar ratio was found to be sufficient for the amount of time required and was used for further tests in experiments.

3.4 Temperature increase due to clathrate hydrate nucleation

When clathrate hydrates begin to nucleate, there is an initial increase in the temperature of the fluid sample before the crystals begin to anneal and form into a solid plug. To determine the expected temperature changes during crystal formation, a 1:5 THF to water solution, without any nanoparticles, was first mixed using the blender before slowly cooling down to -5 , -3 , -2 , 0 , 2 , and 4 °C. By gradually and slowly cooling the samples to these temperatures, we can prolong the time required before initial nucleation of the hydrates begins until the desired temperatures have been reached. Once the temperature was reached, a seed crystal was introduced to induce nucleation. The temperature of the samples was monitored using a digital temperature probe. To compare each set of data, the temperatures recorded were set relative to the initial time of nucleation for each sample. The measurements continued for 40 min to observe the decrease in temperature after the initial increase. These tests were conducted to determine the change in temperature during the nucleation period. The results of these tests can be used to explain the time period between the initial nucleation and the beginning of the agglomeration phase of hydrate growth.

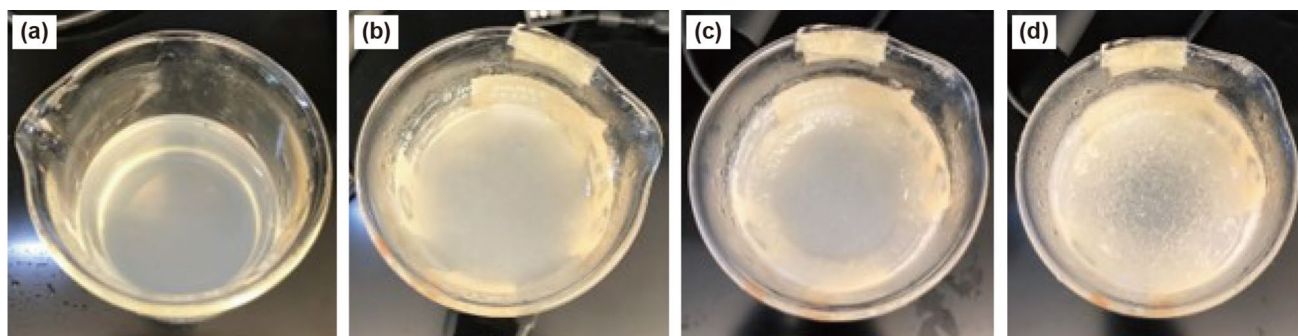


Fig. 5 Progression of hydrate development. **a** Initial SiO₂ dispersion with THF. **b** Initial nucleation of hydrate development. **c** Beginning of hydrate agglomeration. **d** Complete agglomeration of hydrates

3.5 Nucleation times for different nanoparticles

The time which is required to initiate clathrate hydrate crystal nucleation is known as the nucleation time. Once the crystals start to nucleate, it causes a cascade of crystal production throughout the sample where both solid and liquid phases of the solution exist before the agglomeration phase of hydrate growth begins. For these tests, 20:80 THF–water solutions with 1% by weight of each nanoparticle solution were observed at both -6 and 0 °C. This test will be used to identify how each of the four nanoparticles differs by inhibiting the formation of hydrates at two temperatures below the required temperature for THF–water hydrate nucleation.

3.6 Agglomeration times for different nanoparticles

The agglomeration time is the time required for the clathrate hydrates to form a solid plug starting after crystal nucleation has caused a dramatic phase shift in the solution. This period begins when the solid crystals agglomerate at the outer perimeter of their containing flask and expand resulting in the development of a solid hydrate crystal. It is essential to understand how the agglomeration rate is impacted by different nanoparticles. When the hydrates exist in their free crystalline form, the hydrates can flow through subsea production pipes, but the agglomeration process allows the free crystals to begin to grow leading to blockages. Understanding the rate of agglomeration for hydrates is a significant factor when deciding to employ subsea pipe cleaning measures which are typically used to sweep wax depositions. It can be costly to use these techniques because they slow down production, but if the subsea pipes are not regularly cleaned, there is a greater possibility of hydrates completely blocking the flow within the pipes. Each of the tests done to determine the agglomeration times was determined by using the same samples used to find the nucleation time for each nanoparticle solution at -6 and 0 °C.

3.7 Nucleation times for different concentrations of nanoparticles

In testing the capability for each of these nanoparticles to act as a kinetic inhibitor, concentrations from 0.15% to 0.6% by weight of each nanoparticle were tested to determine whether there is an optimal concentration in their applications. Nanoparticles of design can be expensive in their uses. Therefore, optimal concentrations are important for their deployment in field applications. It has been well reported that different concentrations of nanoparticles will affect the rate of clathrate hydrate growth. To fulfill

the kinetic inhibition requirements of $< 1\%$ by weight for the nanoparticle concentrations in each sample, four solutions were tested using 0.15, 0.3, 0.45, and 0.6 percent by weight for each nanoparticle.

3.8 Agglomeration times for different concentrations

The time required to complete the agglomeration process of the free clathrate hydrate crystals was measured using the same nanoparticle solutions tested for nucleation times. Each solution was allowed to continue the hydrate growth process by remaining in the recirculating bath until each sample developed into a solid hydrate crystal at 0 °C. The recorded time-lapse videos were analyzed to find both the total time required for complete agglomeration as well as the rate of growth in cm/h.

4 Results and discussion

4.1 The effect of concentration of THF and type of nanoparticles on nucleation times

The nucleation times for clathrate hydrate development show that with different molar ratios of THF to water, the type of nanoparticles used in the sample will influence the nucleation time. Experimental results show that over this range of THF–water ratios, the SiO_2+A nanoparticles can inhibit the nucleation of hydrates by requiring a longer nucleation time compared to samples using the other three nanoparticles and the control. The difference between the SiO_2+A nanoparticles and the other three nanoparticles used is 27%–58% longer nucleation times for hydrate development as shown in Fig. 6.

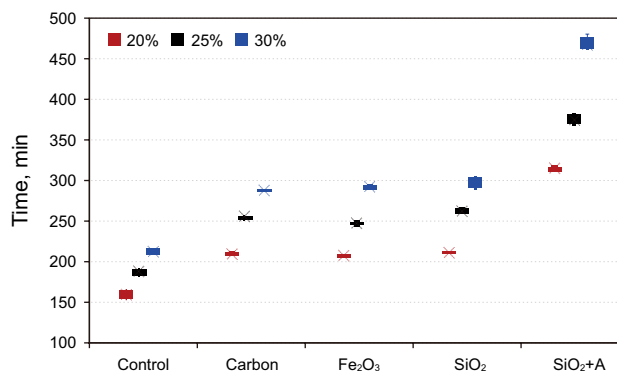


Fig. 6 The time required for clathrate hydrates to nucleate in a solution with 20%–30% (by mole) THF and 70%–80% (by mole) water with 1% by weight of nanoparticles at 0 °C

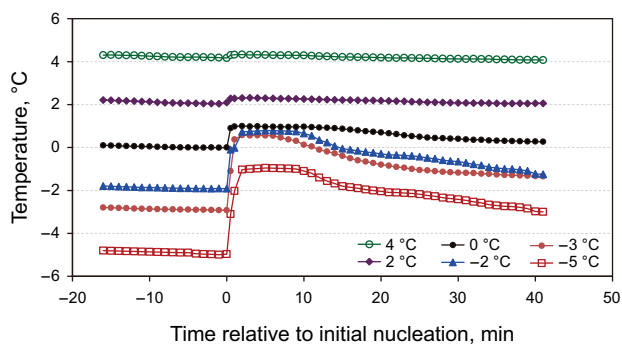


Fig. 7 Increase in temperature due to clathrate hydrates forming in a solution of THF–water (20:80) based on starting temperature when hydrate nucleation begins

4.2 Temperature increase during clathrate hydrate nucleation

When chilling the solutions before inducing hydrate growth, the solutions at lower temperatures produced greater increases in temperatures than those at higher temperatures. As shown in Fig. 7, the samples tested close to the required temperature for nucleation showed a smaller change in temperature after nucleation occurred. The increase in temperature can be predicted to assist in lengthening the amount of time by delaying the onset of the agglomeration period after nucleation compared to if there was no initial increase in temperature.

4.3 Time required for clathrate nucleation using different nanoparticles

As shown in Fig. 8, the nucleation times for each of the carbon, iron III oxide, and silica nanoparticle solutions at 0 °C were very consistent with each other. The SiO₂+A nanoparticle solution provided significantly longer nucleation

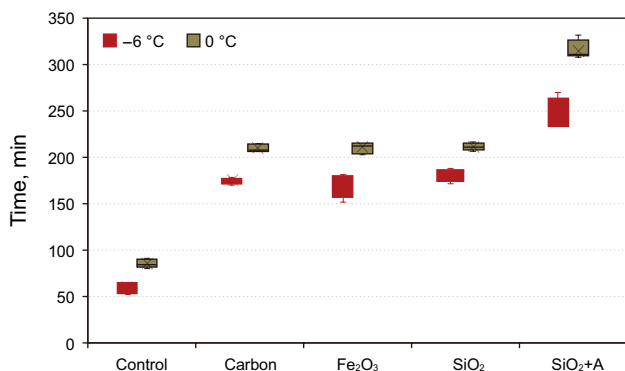


Fig. 8 Effect of temperature on time required to induce clathrate hydrates in a solution of THF–water (20:80) containing 1% by weight of nanoparticles at –6 °C and 0 °C

times than the other three nanoparticle solutions. This very significant increase in nucleation time required for hydrate development for SiO₂+A nanoparticles indicates that the functionalized particles considerably affect the rate of nucleation in the solution. Compared to the other three nanoparticles, the SiO₂+A nanoparticles provided a 43% increase for samples tested at 0 °C and a 30% increase for samples tested at –6 °C in delaying the time required for initial nucleation of hydrate growth.

4.4 Time between nucleation and the agglomeration period to begin

As shown in Fig. 9, there was not a significant difference in the time required for each solution to begin the agglomeration period at 0 and –6 °C. The times observed for each nanoparticle solution show that there is a noticeable increase in the time before agglomeration begins after nucleation being reduced due to the presence of nanoparticles in the solution. The time required for nucleation to occur is crucial, but this period after nucleation when the agglomeration period begins is very important in determining how to manage hydrate growth on subsea equipment when the nucleation period has first been detected. We predict the times between each sample at different temperatures due to the initial increase in temperature of the solution when nucleation occurs.

4.5 Time required for complete clathrate agglomeration using different nanoparticles

There was a significant difference in the agglomeration times for the four nanoparticles at both –6 and 0 °C. At both temperatures, the SiO₂+A nanoparticles performed better than any of the other three nanoparticles shown in Fig. 10. Compared to the trends observed in the nucleation time tests for these samples, the results for the SiO₂ nanoparticles

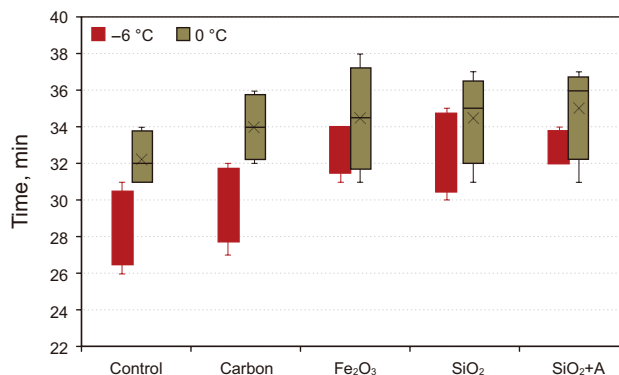


Fig. 9 The time required for the agglomeration period to begin once complete nucleation has occurred for each nanoparticle solution and the control at 0 °C and –6 °C

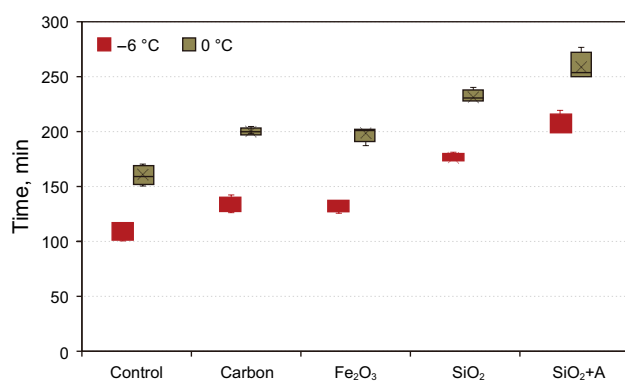


Fig. 10 Effects of temperature on full agglomeration times for THF–water (20:80) clathrate hydrates at 0 and -6 °C containing 1% by weight of nanoparticles

performed nearly as well as the SiO₂+A nanoparticles in slowing the rate of agglomeration. The iron III oxide and carbon nanoparticles continued a similar trend of providing nearly an identical rate of agglomeration. The control sample in this test showed that the presence of nanoparticles did not affect the agglomeration rate as significantly as their presence affect the nucleation rates. Some nanoparticle solutions had very little effect on the agglomeration times (Fig. 10), and the rates are compared (Table 1). The change in the nanoparticle solutions is statistically significant starting at 26% slower agglomeration rates, but these results show that the mechanisms involved with slowing the rates of nucleation and agglomeration are independent of each other in how nanoparticles can affect them.

To better understand the changes in agglomeration times for changing temperatures, the agglomeration rates were calculated and compared between 0 and -6 °C. In Table 1, the rates of agglomeration at different temperatures are listed for each of the four nanoparticle solutions at 1% by weight and the control solution. It is clear that the agglomeration rate is increased when solutions are at lower temperatures. For iron III oxide and carbon nanoparticles, the agglomeration rate at -6 °C is within 7% and 8% of the control samples. Both silicon-based nanoparticles performed significantly better at 32% and 42% reduction in the agglomeration rates from the control for SiO₂ and SiO₂+A, respectively.

Table 1 Agglomeration rates in cm/h of clathrate hydrates of THF–water (20:80) solutions with 1% by weight of nanoparticles at 0 and -6 °C

Temperature, °C	Agglomeration rate, cm/h				
	Control	Carbon	Fe ₂ O ₃	SiO ₂	SiO ₂ +A
0	1.350	1.275	0.872	0.967	0.803
-6	1.771	1.632	1.648	1.201	1.025

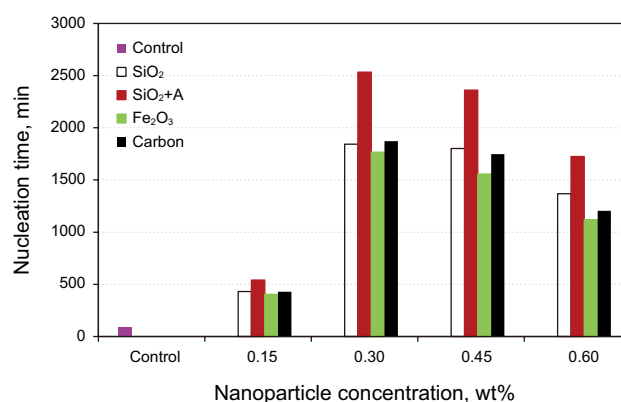


Fig. 11 The time required for THF–water clathrate hydrate nucleation with changing nanoparticle concentrations at 0 °C

4.6 Clathrate nucleation times for different nanoparticle concentrations

The nucleation times required for clathrate hydrate production was significantly increased, as shown in Fig. 11, when comparing the nanoparticle solutions to the control sample. Due to the scale of the graph, the results between each of the four individual tests were averaged and presented in this form to easily distinguish between each nanoparticle. For nanoparticle solutions, the SiO₂+A nanoparticle solutions produced the most considerable change in the required time for clathrate hydrate nucleation. The optimal concentrations for the inhibition of hydrate nucleation were observed to be the greatest for the samples containing 0.30% by weight of nanoparticles. As shown in Fig. 11, when increasing the concentration from 0.15% to 0.30% by weight there was a very significant increase in nucleation time. Samples containing 0.45% by weight of nanoparticles displayed similar results as the samples containing 0.30% by weight of nanoparticles, but the nucleation time began to decrease as the weight percentage of nanoparticles continued to increase.

4.7 Clathrate agglomeration times for different nanoparticle concentrations

Agglomeration times for each nanoparticle solution showed that there was not a significant difference in the agglomeration times at different nanoparticle concentrations (Fig. 12). The SiO₂+A nanoparticles continued to provide the highest increase in agglomeration times compared to the control sample, by increasing the time by an average of 94%. The other three nanoparticles also noticeably increased the agglomeration times by 51%, 52%, and 49% for the carbon, iron III oxide, and SiO₂ nanoparticles, respectively. As with the previous nucleation and agglomeration measurements using 1%

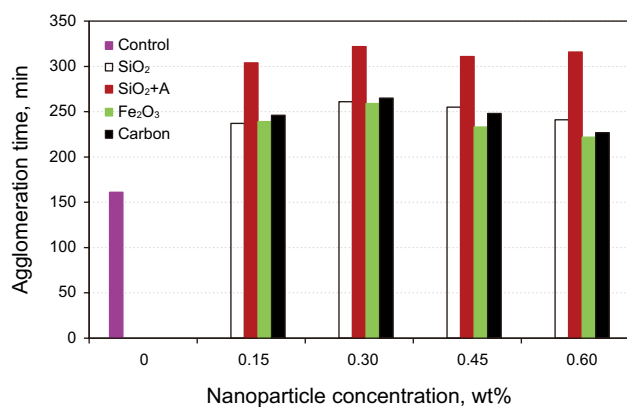


Fig. 12 Agglomeration times of clathrate hydrates of THF–water (20:80) solutions with varying nanoparticle concentrations from 0.15% to 0.60% by weight at 0 °C

Table 2 The average rate of THF–water clathrate hydrate agglomeration in cm/h for each nanoparticle solution at 0 °C

Nanoparticle concentration, wt%	Average agglomeration rate, cm/h				
	Control	SiO ₂	SiO ₂ +A	Fe ₂ O ₃	Carbon
0.00	1.290				
0.15		0.940	0.673	0.833	0.857
0.30		0.782	0.633	0.787	0.770
0.45		0.800	0.656	0.879	0.826
0.60		0.846	0.647	0.919	0.902

by weight of nanoparticles, there was a continued trend that the agglomeration rates were more affected by the type of nanoparticles used, showing that the functionalized SiO₂+A nanoparticles provided a greater inhibition compared to the other three nanoparticles. This increase in inhibition also does not appear to be related to the concentration of nanoparticles in each sample but the presence and the type of nanoparticle used.

To further analyze these results for agglomeration times, the dimensions of the beakers that the hydrates were grown in were used to calculate the average agglomeration rate for each of the five samples. After converting the agglomeration times to agglomeration rates, it became very apparent that the amino-coated SiO₂ nanoparticles had a significant effect on the rate of hydrate agglomeration, as shown in Table 2. The ideal concentration of nanoparticles had already been determined to be 0.30% by weight from the previous analysis, and the difference from the control samples was a 51% reduction in the rate of agglomeration. Each of the other nanoparticles showed that each provided significant reductions in agglomeration rate between 27% and 40%.

5 Conclusions

1. The use of nanoparticles as a kinetic inhibitor of hydrate growth significantly increases the times required for hydrate nucleation and agglomeration to begin, and the required time for complete agglomeration of THF–water hydrate clathrates.
2. Compared to a control without nanoparticles, the time required for nucleation of THF–water hydrate clathrates significantly increases when nanoparticles are added to THF–water solutions. At 0.15% by weight of nanoparticles, we observed an increase in the time required for nucleation to begin. The greatest increase was found at 0.30% by weight of nanoparticles compared to the control. As the nanoparticle weight percent increases beyond 0.30, the time required before hydrates begin to develop decreases.
3. Amino-coated SiO₂ nanoparticles outperform all other nanoparticles when used as an additive for inhibiting the growth of clathrate hydrates. With comparable concentrations in solutions, these nanoparticles provide an increase in the nucleation times for clathrate hydrates.
4. At the moment of THF and water clathrate hydrates induction, there is a sudden and increasingly significant rise in temperature within the solution. We predict that this increase in temperature when nucleation begins will affect the time required for the agglomeration period to begin.
5. For preventing methane hydrates, it is recommended based on our findings using THF–water clathrates as a model that amino-coated SiO₂ nanoparticles, and potentially other amino-coated nanoparticles, can be used as very effective hydrate inhibitors. The presence of nanoparticles at 0.30% by weight will cause a significant increase in the nucleation time, increase the time before agglomeration, and increase the total time before the agglomeration period commences.

Open Access This article is distributed under the terms of the Creative Commons Attribution 4.0 International License (<http://creativecommons.org/licenses/by/4.0/>), which permits unrestricted use, distribution, and reproduction in any medium, provided you give appropriate credit to the original author(s) and the source, provide a link to the Creative Commons license, and indicate if changes were made.

References

- Abay H. Kinetics of gas hydrate nucleation and growth. Ph.D Dissertation. The University of Stavanger. 2011.
- Agarwal S, Phuoc TX, Soong Y, Martello D, Gupta RK. Nanoparticle-stabilized invert emulsion drilling fluids for deep-hole

- drilling of oil and gas. *Can J Chem Eng.* 2013;91(10):1641–9. <https://doi.org/10.1002/cjce.21768>.
- Amanullah M, Al-Tahini AM. Nano-technology: Its significance in smart fluid development for oil and gas field application. In: SPE Saudi Arabia section technical symposium. Al-Khobar, Saudi Arabia; 9–11 May 2009. <https://doi.org/10.2118/126102-MS>.
- Ameripour S. Prediction of gas-hydrate formation conditions in production and surface facilities. Thesis. Texas A&M University, USA. 2005.
- Anderson BJ, Tester JW, Borghi GP, Trout BL. Properties of inhibitors of methane hydrate formation via molecular dynamics simulations. *J Am Chem Soc.* 2005;127(50):17852–62. <https://doi.org/10.1021/ja0554965>.
- Birkedal KA. Hydrate Formation and CH₄ production from natural gas hydrates. MS Thesis. The University of Bergen. 2009.
- Bishnoi PR, Dholabhai PD. Equilibrium conditions for hydrate formation for a ternary mixture of methane, propane and carbon dioxide, and a natural gas mixture in the presence of electrolytes and methanol. *Fluid Phase Equilib.* 1999;158–160:821–7. [https://doi.org/10.1016/S0378-3812\(99\)00103-X](https://doi.org/10.1016/S0378-3812(99)00103-X).
- Catak E. Hydrate dissociation during drilling through in situ hydrate formations. Thesis. Louisiana State University and Agricultural and Mechanical College. 2006.
- Grover T. Natural gas hydrates—Issues for gas production and geomechanical stability. Ph.D Dissertation. Texas A&M University. 2008.
- Halliday W, Clapper DK, Smalling M. New gas hydrate inhibitors for deepwater drilling fluids. In: IADC/SPE drilling conference 3–6 Mar, Dallas TX, 1998. <https://doi.org/10.2118/39316-MS>.
- Kim NR, Ribeiro PR, Bonet EJ. Study of hydrate in drilling operations: a review. In: 4th PDPETRO Campinas SP Oct 2007.
- Kjaer KL. Well control considerations in arctic drilling. Thesis. The University of Stavanger. 2014.
- Lee JY, Yun TS, Santamarina JC, Ruppel C. Observations related to tetrahydrofuran and methane hydrates for laboratory studies of hydrate-bearing sediments. *Geochem Geophys Geosyst.* 2007;8(6):Q06003. <https://doi.org/10.1029/2006GC001531>.
- Li XS, Xu CG, Chen ZY, Wu HJ. Hydrate-based pre-combustion carbon dioxide capture process in the system with tetra-*n*-butyl ammonium bromide solution in the presence of cyclopentane. *Energy.* 2011;36(3):1394–403. <https://doi.org/10.1016/j.energy.2011.01.034>.
- Meindinyo, R. Gas hydrate growth kinetics. Ph.D Dissertation. The University of Stavanger. 2017.
- Nesterov AN, Reshetnikov AM. Promotion and inhibition of gas hydrate formation by oxide powders. *J Mol Liq.* 2015;204:118–25. <https://doi.org/10.1016/j.molliq.2015.01.037>.
- Pakulski M. Development of superior hybrid gas hydrate inhibitors. In: Offshore technology conference (OTC-21747-MS.), 2–5 May 2011.
- Sloan ED Jr. *Clathrate Hydrates of Natural Gases*. New York: Marcel Dekker; 1990.
- Taurozzi JS, Hackley VA, Wiesner MR. Preparation of nanoparticle dispersions from powdered material using ultrasonic disruption. Gaithersburg: NIST Special Publication; 2012. p. 1200–2.
- Wang ZY, Yu J, Zhang JB, et al. Improved thermal model considering hydrate formation and deposition in gas-dominated systems with free water. *Fuel.* 2019;236:870–9. <https://doi.org/10.1016/j.fuel.2018.09.066>.
- Xu CG, Zhang SH, Cai J, Chen ZY, Li XS. CO₂ (carbon dioxide) separation from CO₂–H₂ (hydrogen) gas mixtures by gas hydrates in TBAB (tetra-*n*-butyl ammonium bromide) solution and Raman spectroscopic analysis. *Energy.* 2013;59:719–25. <https://doi.org/10.1016/j.energy.2013.07.056>.
- Zerpa L. A practical model to predict gas hydrate formation dissociation and transportability in oil and gas flowlines. Dissertation. Colorado School of Mines. 2013.